Preprints of the 21st IFAC World Congress (Virtual)
Berlin, Germany, July 12-17, 2020

Gait Control of a Fully Actuated Walking Robot ⋆

Sally Hui * **Mohamed Al Lawati** ** **Mireille E. Broucke** *

* *Dept. of Electrical and Computer Engineering, University of Toronto, Canada (e-mail: broucke@control.utoronto.ca).*
** *University of Alberta, Canada.*

Abstract: This paper considers the problem of feedback control of a fully actuated biped robot such that a virtual holonomic constraint (VHC) is enforced concomitant with control of the stance leg using a reach control methodology. The reach controller achieves safety and liveness specifications on the stance leg speed and the step size, resulting in a polytopic state space for the restricted hybrid dynamics on the VHC constraint manifold. It is shown that both the restricted system and the full hybrid system exhibit a stable, hybrid limit cycle. The design method can provide a way to compliantly adjust gait speed, for instance, to gently transition between different gaits, while maintaining transients within safe bounds.

Keywords: Walking robots, virtual holonomic constraints, reach control theory

1. INTRODUCTION

Interest in the design of walking robots has exploded in the last decade with significant theoretical and practical advances. Many recent designs focus on underactuated robots because actuators are costly, underactuated robots may better mimic the passive walking of humans, and because they present an exciting challenge to control theorists. However, even for fully actuated robots, the entire enterprise rests on overcoming robustness issues: to achieve stable motion in the face of variable terrains (Agrawal and Sreenath, 2019), unmodeled loads, foot slippage (Clark and Bloch, 2018), transitions between gaits (Da et al., 2016), and other disturbances.

With this perspective, we consider the problem of how to compliantly adjust the speed of a gait, what we call "gait control", for a fully actuated walking robot. We assume the gait has already been designed in the form of a virtual holonomic constraint (VHC) (Grizzle et al., 2001; Westervelt et al., 2002, 2003; Freidovich et al., 2008; Otsason and Maggiore, 2019). The VHC enforces an algebraic relationship between the swing and stance leg angles. In the fully actuated case, this leaves the time evolution of the stance leg - more simply, the gait speed - as the remaining design variable.

In the VHC literature, the gait speed may be regulated through foot placement at the end of a step, and this ties the gait speed to the VHC itself. This leads to a method of "gain scheduling" gaits to achieve a speed profile (Westervelt et al., 2007; Da et al., 2016). We asked the question: in the fully actuated case, could "gentle" regulation of the stance leg contribute to the robustness of the overall design? We started with safety and liveness specifications for the stance leg which arise in current platforms such as the Cassie robot (Gong et al., 2019). Inspired by a reach control approach (Habets et al., 2006; Roszak and Broucke, 2006; Kloetzer and Belta, 2008; Broucke, 2010; Helwa and Broucke, 2013), we propose a simple controller to achieve the specifications on the restricted stance leg dynamics (the dynamics on the VHC constraint manifold) such that the restricted system evolves in a polytopic region $\mathcal{P}$ determined by the specifications, even during transients (such as during gait transitions). The gait speed emerges as an artifact of a stable hybrid limit cycle.

The only part of our design that relies on simulations is the estimation of the domain of positive invariance of the polytopic state space $\mathcal{P}$ for the full hybrid model. Here numerical procedures to estimate domains of attraction of hybrid limit cycles can provide complementary tools (Manchester et al., 2010). In summary, we present a design procedure and theoretical results that are conceptually extendable to other fully actuated robot configurations (whose models are feedback linearizable) and which may offer a way to transition between gait speeds in a compliant, gentle manner, to the benefit of robustness of the overall design.

2. MODEL OF BIPED WALKER

We consider a fully actuated two degree of freedom (2DOF) biped walker consisting of two legs, a hip, and two feet. Referring to Figure 1, q_1 and q_2 are the angles of the legs with respect to a vertical, the masses of the legs are $m_1 = m_2$, the moments of inertia about the centers of mass are $I_1 = I_2$, the length of each leg is l, and $l_1 + l_2 = l$, where l_1 is the length from the foot to the center of mass of each leg. The leg touching the ground is called the *stance leg*, and the other leg is called the *swing leg*.

Using the Euler-Lagrange formulation, we obtain the standard model for the continuous time dynamics

$$M(q)\ddot{q} + C(q,\dot{q})\dot{q} + G(q) = B(q)u\,, \qquad (1)$$

⋆ Supported by the Natural Sciences and Engineering Research Council of Canada (NSERC) and Sultan Qaboos University (SQU).

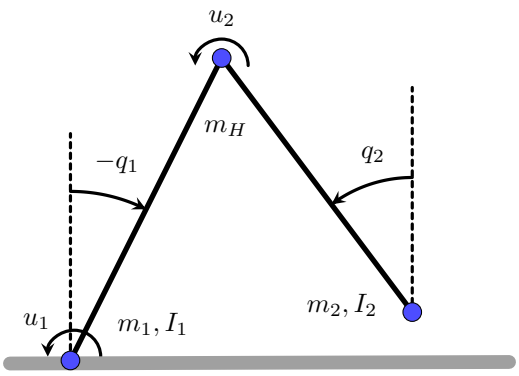

Fig. 1. The 2DOF biped walker.

where $q \in \mathbb{R}^2$ are the generalized coordinates, $u \in \mathbb{R}^2$ is the input, and

$$M(q) = \begin{bmatrix} m_1 l_1^2 + m_2 l^2 + m_H l^2 + I_1 & m_2 l l_2 \cos(q_1 - q_2) \\ m_2 l l_2 \cos(q_1 - q_2) & m_2 l_2^2 + I_2 \end{bmatrix}$$
$$C(q, \dot{q}) = \begin{bmatrix} 0 & m_2 l l_2 \sin(q_1 - q_2)\dot{q}_2 \\ -m_2 l l_2 \sin(q_1 - q_2)\dot{q}_1 & 0 \end{bmatrix}$$
$$G(q) = \begin{bmatrix} (m_1 g l_1 + m_H g l + m_2 g l)\cos(q_1) \\ m_2 g l_2 \cos(q_2) \end{bmatrix}, \; B = \begin{bmatrix} 1 & -1 \\ 0 & 1 \end{bmatrix}.$$

The model (1) captures the continuous time dynamics of the biped walker. During a gait cycle, the swing leg hits the ground at two points: first, when it passes the stance leg, namely when $q_2 = q_1$; and second, when $q_2 = -q_1$. Similar to other researchers, we assume no impact occurs when the swing leg passes the stance leg (see (Grizzle et al., 2001) for a discussion on methods for the swing leg to avoid scuffing the ground). To model the impact of interest, we define $H(q) := \cos(q_1) - \cos(q_2)$ for the height of the swing leg. Then the *switching surface* characterizes that the swing leg is descending at the moment of impact, as given by

$$\mathcal{S} = \left\{ (q, \dot{q}) \in \mathbb{R}^{2n} \mid q_2 = -q_1 \,, \quad \frac{\partial H(q)}{\partial q}\dot{q} < 0 \right\}. \tag{2}$$

When an impact occurs, the stance and swing legs switch roles; hence, q_1 and q_2 must be swapped. Additionally, $\dot{q}_1$ and $\dot{q}_2$ are reset according to the principle of conservation of angular momentum. The result is that both q and $\dot{q}$ are reset after an impact according to a *reset map*

$$\begin{bmatrix} q^+ \\ \dot{q}^+ \end{bmatrix} = J(q, \dot{q}) \tag{3}$$

where the $+$ superscript indicates values just after an impact event. In summary, the state of the biped model is $(q_1, q_2, \dot{q}_1, \dot{q}_2) \in \mathbb{R}^4$, and (1) and (3) together define a hybrid system.

3. VIRTUAL HOLONOMIC CONSTRAINT

A *virtual holonomic constraint* (VHC) is a relation $h(q) = 0$ where $h : \mathbb{R}^n \to \mathbb{R}^m$ is smooth (in this paper $m = 1$) and $\operatorname{rank}(dh_q) = m$ for all $q \in h^{-1}(0)$. The *constraint manifold* associated with a VHC is defined as

$$\Gamma := \{(q, \dot{q}) \in \mathbb{R}^{2n} \mid h(q) = 0 \text{ and } \frac{\partial h(q)}{\partial q}\dot{q} = 0\}.$$

Generally, the control problem associated with a VHC is to design a feedback controller such that Γ is positively invariant and asymptotically stable.

For the 2DOF walker studied in this paper, the VHC takes the form

$$h(q_1, q_2) := q_2 - p(q_1) \tag{4}$$

where $p : [0, 2\pi) \to \mathbb{R}$. The choice of p is informed by the requirements on a normal gait cycle such that the center of mass of the hip moves monotonically in one direction. First, the stance leg must continuously "fall forward", passing through the upright position during a gait cycle. Mathematically, the angle q_1 is positive at the start of a step, passes through zero, and becomes negative before an impact event. In order to achieve a regular gait, it is reasonable to assume the impact event when the height of the swing leg is decreasing is associated with a unique negative value of the stance leg angle. That is, there exists a unique number $q_1^* < 0$ satisfying $q_1^* + p(q_1^*) = 0$ such that if $(q, \dot{q}) \in \mathcal{S} \cap \Gamma$, then $q_1 = q_1^*$.

Figure 2 depicts a VHC for a normal gait with p realized as a polynomial; a similar VHC was employed in (Freidovich et al., 2008). We observe from the figure that when the VHC is enforced, the gait step begins in the lower right endpoint of the curve when $q_2 = -q_1$ (both legs touching the ground), and it ends at the upper left endpoint when again $q_2 = -q_1$, with the step progressing according to movement from the right of the figure to the left.

The discrete phase of the hybrid dynamics is captured by the dashed line in the figure, representing the switching surface $\mathcal{S}$. When the states reach the upper left endpoint with $q_2 = -q_1$, they are reset back to the lower right endpoint according to the reset (3). In order for the VHC to remain enforced after the reset, we require that

$$q_2^+ = p(q_1^+), \quad \dot{q}_2^+ = \left.\frac{\partial p(q_1)}{\partial q_1}\right|_{q_1^+} \dot{q}_1^+ . \tag{5}$$

Collecting all information about $\mathcal{S}$ and Γ, (5) reduces to conditions on p: for all $(q, \dot{q}) \in \mathcal{S} \cap \Gamma$,

$$p(q_1) = -p(-q_1) \tag{6}$$
$$\frac{\partial p(q_1)}{\partial q_1}|_{q_1^+} = \left[\hat{J}_{11} + \hat{J}_{12} \left.\frac{\partial p(q_1)}{\partial q_1}\right|_{q_1}\right]^{-1} \left[\hat{J}_{21} + \hat{J}_{22} \left.\frac{\partial p(q_1)}{\partial q_1}\right|_{q_1}\right] \tag{7}$$

Under the additional constraints (6) and (7), we say the VHC (4) is a *hybrid virtual holonomic constraint*.

We perform a global coordinate transformation in order to decompose the model into dynamics off the constraint manifold Γ induced by the VHC and the dynamics on Γ (such a decomposition is feasible because the constraint manifold will be rendered positively invariant by a suitable feedback). Let $\xi := (\xi_1, \xi_2)$ and $\eta := (\eta_1, \eta_2)$ and define the transformation $(\xi, \eta) := T(q, \dot{q}) = (q_2 - p(q_1), \dot{q}_2 - \frac{\partial p(q_1)}{\partial q_1}\dot{q}_1, q_1, \dot{q}_1)$. Then the system (1) takes the form

$$\begin{aligned} (\dot{\xi}, \dot{\eta}) &= \hat{f}(\xi, \eta) + \hat{g}(\xi, \eta)u \qquad \text{if } (\xi, \eta) \notin \hat{\mathcal{S}} \\ (\xi^+, \eta^+) &= \hat{J}(\xi, \eta) \qquad\qquad\quad \text{if } (\xi, \eta) \in \hat{\mathcal{S}} \end{aligned} \tag{8}$$

for suitable functions $\hat{f}$ and $\hat{g}$; the details of $\hat{J}$ are given below. The switching surface is

$$\hat{\mathcal{S}} = T(\mathcal{S}) = \{(\xi, \eta) \in \mathbb{R}^4 \mid \xi_1 = -p(\eta_1) - \eta_1 \,, \dot{\hat{H}} < 0\}, \tag{9}$$

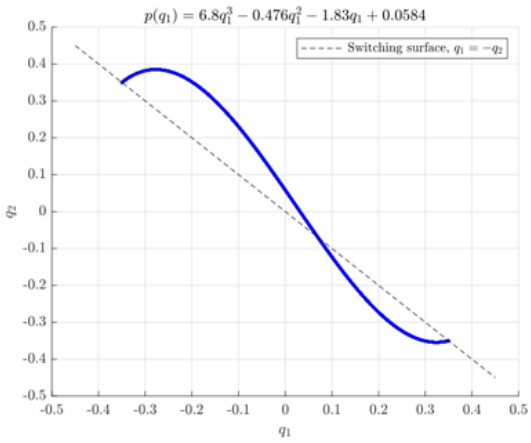

Fig. 2. A typical gait shape.

where $\dot{\hat{H}}$ is the Lie derivative of the height function in new coordinates. Similarly, the constraint manifold becomes

$$\hat{\Gamma} \coloneqq \{(\xi, \eta) \in \mathbb{R}^4 \mid \xi = 0\}\,. \tag{10}$$

In the last modeling step, we feedback linearize the model (8) by applying the feedback control

$$u = A_1^{-1}(x)\Big|_{x=T^{-1}(\xi,\eta)} \begin{bmatrix} -L_f^2 h_1(x)\Big|_{x=T^{-1}(\xi,\eta)} + v_1 \\ -L_f^2 h_2(x)\Big|_{x=T^{-1}(\xi,\eta)} + v_2 \end{bmatrix} \tag{11}$$

where $h_1(q_1, q_2) \coloneqq h(q_1, q_2) = q_2 - p(q_1)$ and $h_2(q_1, q_2) \coloneqq q_1$, v_1 and v_2 are two auxiliary control inputs, and the $(i,j)^{\text{th}}$ entry of $A_1(x) \in \mathbb{R}^{2\times 2}$ is $L_{g_j} L_f h_i(x)$. Under the feedback (11), system (8) becomes

$$\begin{aligned} &\dot{\xi}_1 = \xi_2 \qquad \dot{\eta}_1 = \eta_2 \qquad \text{if } (\xi,\eta) \notin \hat{\mathcal{S}} \\ &\dot{\xi}_2 = v_1 \qquad \dot{\eta}_2 = v_2 \\ &(\xi^+, \eta^+) = \hat{J}(\xi, \eta) \qquad \text{if } (\xi,\eta) \in \hat{\mathcal{S}}\,, \end{aligned} \tag{12}$$

where the reset map $\hat{J}(\xi, \eta)$ for $(\xi, \eta) \in \hat{\mathcal{S}}$ is given by

$$\xi_1^+ = \eta_1 - p(-\eta_1) \tag{13a}$$
$$\xi_2^+ = \beta(\eta_1)\xi_2 + \alpha(\eta_1)\eta_2 \tag{13b}$$
$$\eta_1^+ = -\eta_1 \tag{13c}$$
$$\eta_2^+ = \gamma(\eta_1)\eta_2 + \mu(\eta_1)\xi_2\,, \tag{13d}$$

and

$$\begin{aligned} \alpha(\eta_1) \coloneqq{}& \hat{J}_{21}(\eta_1) + \hat{J}_{22}(\eta_1)\, \frac{\partial p}{\partial \eta_1}\Big|_{\eta_1} \\ &- \frac{\partial p}{\partial \eta_1}\Big|_{-\eta_1} \left(\hat{J}_{11}(\eta_1) + \hat{J}_{12}(\eta_1)\, \frac{\partial p}{\partial \eta_1}\Big|_{\eta_1}\right) \end{aligned} \tag{14a}$$

$$\beta(\eta_1) \coloneqq \hat{J}_{22}(\eta_1) - \hat{J}_{12}(\eta_1)\, \frac{\partial p}{\partial \eta_1}\Big|_{-\eta_1} \tag{14b}$$

$$\gamma(\eta_1) \coloneqq \hat{J}_{11}(\eta_1) + \hat{J}_{12}(\eta_1)\, \frac{\partial p}{\partial \eta_1}\Big|_{\eta_1} \tag{14c}$$

$$\mu(\eta_1) \coloneqq \hat{J}_{12}(\eta_1)\,. \tag{14d}$$

We observe that the role of the ξ dynamics is to enforce the VHC. Instead the η dynamics capture the dynamics of the stance leg since $\eta = (q_1, \dot{q}_1)$.

4. PROBLEM STATEMENT

Consider the VHC (4) transformed into (ξ, η) coordinates:

$$h(\xi) \coloneqq \xi_1\,. \tag{15}$$

Assumption 1. We impose the following assumptions.

(A1) The map $p : [0, 2\pi) \to \mathbb{R}$ is smooth.
(A2) There exists a unique $\eta_1^\star < 0$ such that $\eta_1^\star + p(\eta_1^\star) = 0$. Moreover, there exist $\varepsilon_1 > 0$ and $L_\eta > 0$ such that for all η_1 with $|\eta_1 + p(\eta_1)| < \varepsilon_1$, $|\eta_1 - \eta_1^\star| < L_\eta |\eta_1 + p(\eta_1)|$.
(A3) $p(-\eta_1^\star) = -p(\eta_1^\star)$.
(A4) $\alpha(\eta_1^\star) = 0$.
(A5) $\left|1 + \frac{\partial p}{\partial \eta_1}\Big|_{-\eta_1^\star}\right| < \left|1 + \frac{\partial p}{\partial \eta_1}\Big|_{\eta_1^\star}\right|$.

Remark 2. Assumption (A1) is immediate since we work with polynomial functions for p. Assumptions (A3) and (A4) reiterate our findings in (6) and (7) ensuring invariance of the VHC over a discrete step. Assumption (A5) will be used to show that $\xi(t)$ does not grow over a discrete step. Finally, Assumption (A2) regards the graph of the polynomial with respect to the switching surface; it is best visualized using Figure 2. In that figure we see that there is a unique point $\eta_1^\star < 0$ when $p(\eta_1^\star)$ and the switching surface $\hat{\mathcal{S}}$ intersect; that is, when $p(\eta_1^\star) - (-\eta_1^\star) = 0$. Near $\eta_1^\star$, $p(\eta_1)$ is concave up. Now the vertical distance between $p(\eta_1)$ and the switching surface $-\eta_1$ is $|\eta_1 + p(\eta_1)|$. Assumption (A2) states there is a lower bound on the slope $\frac{|\eta_1 + p(\eta_1)|}{|\eta_1 - \eta_1^\star|}$ near $\eta_1^\star$. ◁

Problem 3. Consider the hybrid system consisting of the feedback linearized model (12), the switching surface (9), and the reset map (13). Suppose we have a VHC (15) satisfying Assumption 1.

Let c_i, $i = 1, \ldots, 4$ be positive constants such that $-c_1 < \eta_1^* < 0$. We want to find decoupled feedback controllers $v(\xi, \eta) = (v_1(\xi), v_2(\eta))$ such that the closed-loop system consisting of (1), the feedback linearizing controller (11), and the feedback $v(\xi, \eta)$ satisfies the following specifications:

(i) **VHC**: The constraint manifold $\hat{\Gamma}$ is positively invariant and asymptotically stable over the continuous evolution of (12), and it is invariant over the discrete transitions of (12).
(ii) **Liveness**: The stance leg angular velocity is bounded away from zero. That is, $\eta_2 \le -c_3 < 0$.
(iii) **Safety**: The size of any step of the stance leg is bounded. That is, $-c_1 \le \eta_1 \le c_2$. The stance leg angular velocity is bounded. That is, $|\eta_2| \le c_4$.
(iv) **Regular Gait**: For a regular gait, $\eta_1(t)$ decreases monotonically over its continuous evolution from a positive to a negative value.

Specification (i) is achievable, firstly, due to the constraints (6) and (7), and secondly by using a pole placement controller for the auxiliary input v_1 in order to null the ξ dynamics. This part of the design will be discussed only briefly. The specifications (ii)-(iv), which regard the design of v_2 to control the stance leg, are discussed next.

5. CONTROL DESIGN

Consider the η dynamics given in (12). Our design methodology is inspired by a reach control approach (Habets et al., 2006; Roszak and Broucke, 2006; Kloetzer and Belta, 2008; Broucke, 2010; Helwa and Broucke, 2013). The first step of the design is to identify a polytopic state space $\mathcal{P}$. In the present case, $\mathcal{P}$ arises directly from our safety and liveness specifications:

$$\mathcal{P} = \left\{\eta \in \mathbb{R}^2 \mid -c_1 \leq \eta_1 \leq c_2\,,\ \eta_2 \leq -c_3\,,\ |\eta_2| \leq c_4\right\}.$$

The reach control approach involves triangulating $\mathcal{P}$ and designing affine controllers on each simplex so that the control specifications are met. Given the simplicity of both $\mathcal{P}$ and the double integrator dynamics of η, the state space can be easily triangulated and one can find affine controllers such that the stance angle η_1 is mononotically decreasing and $\mathcal{P}$ is positively invariant under the hybrid dynamics. Figure 3 shows such a triangulation.

Suppose we take the specific reach controller

$$v_2(\eta) = [0\ K_2]\,\eta + g\,, \tag{16}$$

where $K_2 = -2.4$ and $g = -1.4$. It has been designed by selecting the velocity vectors at the vertices of $\mathcal{P}$ and then affinely extending those values using the procedure in (Habets et al., 2006; Roszak and Broucke, 2006). Note that since we use the same affine controller in each simplex, the choice of triangulation is effectively arbitrary. The closed-loop η dynamics are

$$\dot{\eta} = \begin{bmatrix} 0 & 1 \\ 0 & K_2 \end{bmatrix} \eta + \begin{bmatrix} 0 \\ g \end{bmatrix}. \tag{17}$$

We examine five properties of (17). First, as can be seen in Figure 3, all solutions leave $\mathcal{P}$ in finite time through the left face of $\mathcal{P}$, and not through its upper, lower, or right faces. Second, while $\mathcal{P}$ clearly has no equilibria, it does contain an invariant affine space under (17) given by

$$\mathcal{W} := \{\eta \in \mathbb{R}^2 \mid \eta_2 = -g/K_2\}.$$

Shifting $\mathcal{W}$ up or down is the mechanism by which the gait speed is calibrated. Particularly, the reach controller induces a unique hybrid limit cycle in $\mathcal{P}$, and this hybrid limit cycle can shifted up and down in $\mathcal{P}$ by shifting $\mathcal{W}$ in the same direction. A hybrid limit cycle higher in $\mathcal{P}$ corresponds to a longer period, and vice versa. The period of the limit cycle determines the gait speed that we seek to influence.

For the third property, denote the point to set distance from a point η to $\mathcal{W}$ by $d_{\mathcal{W}}(\eta) := \min_{w\in\mathcal{W}} \|\eta - w\|$, and let $\eta(t)$ be a solution of (17). Then by standard properties of linear systems

$$d_{\mathcal{W}}(\eta(t)) = \mathrm{e}^{K_2 t} d_{\mathcal{W}}(\eta(0))\,. \tag{18}$$

The fourth property of (17) is that the time T for solutions of (17) to cross $\mathcal{P}$ starting from a vertical segment $\mathcal{V}$ in $\mathcal{P}$ and ending in another vertical segment $\mathcal{V}'$ satisfies:

$$\forall \eta_0, \eta_0' \in \mathcal{V}\,,\ \eta_{0,2} < \eta_{0,2}' \implies T < T' \tag{19}$$

where T and T' are the times for the solutions starting at η_0 and η_0', respectively, to cross from $\mathcal{V}$ to $\mathcal{V}'$. This immediately follows from the fact that $\dot{\eta}_1 = \eta_2$, so more negative values of η_2 imply larger negative velocities of η_1. Finally, the fifth property again regards the crossing time. Define the cross sections

$$\mathcal{V}^- = \{\eta \in \mathcal{P} \mid \eta_1 = \eta_1^\star\}\,,\ \mathcal{V}^+ = \{\eta \in \mathcal{P} \mid \eta_1 = -\eta_1^\star\}\,. \tag{20}$$

There exists a minimum time $T^\star$ for solutions of (17) to cross from $\mathcal{V}^+$ to $\mathcal{V}^-$. This minimum time depends on the safety constraint $|\eta_2| \leq c_4$.

We summarize the salient properties of our design. Let $\lambda_1 < 0$, and $K_2 < 0$ be given. For any solution $(\xi(t), \eta(t))$, define $t^0 := 0$ and let $\{t^k\}$, $k \geq 1$, be the sequence of switching times. We adopt the notational convention that $(\xi(t^0)^+, \eta(t^0)^+) = (\xi(t^0), \eta(t^0))$. Denote the time intervals $T^k := t^k - t^{k-1}$, $k \geq 1$. Let $T^\star$ be the minimum time for solutions of (17) to cross from $\mathcal{V}^-$ to $\mathcal{V}^+$. We can find decoupled controllers (v_1, v_2) and a set of initial conditions $\Omega_0 \subset \mathbb{R}^2 \times \mathcal{P}$ such that for each solution $(\xi(t), \eta(t))$ with $(\xi(0), \eta(0)) \in \Omega_0$ the following hold:

(C1) There exists a monotonically increasing sequence of times $\{t^k\}$ such that $(\xi(t^k), \eta(t^k)) \in \hat{\mathcal{S}}$, $\eta_1^\star \leq \eta_1(t^k) < 0$, and $T^{k+1} > T^\star$, for all $k \geq 1$. Also, $(\xi(t), \eta(t)) \in \mathcal{P}$ for all $t \in [t^{k-1}, t^k]$ and $k \geq 1$.

(C2) For all $k \geq 1$ and $t \in [t^{k-1}, t^k]$, $d_{\mathcal{W}}(\eta(t)) = \mathrm{e}^{K_2 t} d_{\mathcal{W}}(\eta(t^{k-1})^+)$, where $\mathcal{W}$ is an invariant affine space of (17).

(C3) For all $k \geq 1$ and $t \in [t^{k-1}, t^k]$, $\|\xi(t)\| \leq \mathrm{e}^{\lambda_1 t}\|\xi(t^{k-1})^+\|$.

Remark 4. Property (C1) is a non-blocking requirement that places restrictions on the initial condition set Ω_0 to guarantee that $\eta(t)$ continues to evolve in $\mathcal{P}$; that is, the robot continues to take a next step. It includes a mild condition that $T^{k+1} \geq T^\star$, which may be verified in simulation or may be met by reducing $T^\star$. One can prove existence of a stable hybrid limit cycle without this assumption; we opted for simpler theoretical arguments here. (C1) is the only property that must be verified in simulation; however, an (analytically obtained) estimate of Ω_0 is available based on the hybrid η dynamics alone (see the design procedure in Section 7). The other properties are provably satisfied for the selected controllers: property (C2) reiterates the analysis above for v_2 regarding the invariant affine space $\mathcal{W}$. Property (C3) can be achieved using a pole placement controller for v_1. ◁

6. HYBRID LIMIT CYCLE

The goal of this section is to prove that our design realizes a unique, stable hybrid limit cycle. For background on solutions of hybrid systems, hybrid limit cycles, and their stability, the reader is referred to (Westervelt et al., 2007). First Lemmas 5 and 6 establish the exponential stability of the hybrid ξ dynamics. For the next result, a partial argument appeared in (Al Lawati and Yousef, 2016); we give the complete proof in Appendix A.

Lemma 5. Consider the hybrid system (12), and suppose that Assumption 1 holds. There exists $\varepsilon_2 > 0$ such that for all $(\xi, \eta) \in \hat{\mathcal{S}}$, if $|\eta_1 - \eta_1^\star| < \varepsilon_2$, then $|\xi_1^+| < |\xi_1|$, where ξ_1^+ is given by (13a).

We know by property (C3) that the ξ dynamics are exponentially stable over their continuous evolution. This exponential decay must be balanced with the growth of ξ over a discrete step. Lemma 5 proposes the condition (A2) on the VHC to guarantee contraction of $|\xi_1|$ over a discrete step. It remains to contend with the growth of

$|\xi_2|$. Its growth over a discrete step is determined by (13b); particularly $\beta(\cdot)$ and $\alpha(\cdot)$. Since these are $\mathcal{C}^1$ functions, we can bound their growth using Lipschitz constants near $\eta_1^\star$. To that end, let $L_\alpha > 0$ be such that for all η_1, η_1' with $|\eta_1 - \eta_1^\star| < \varepsilon_2$ and $|\eta_1' - \eta_1^\star| < \varepsilon_2$, we have $|\alpha(\eta_1) - \alpha(\eta_1')| \leq L_\alpha |\eta_1 - \eta_1'|$.

Lemma 6. Consider the hybrid system (12), and suppose that Assumption 1 holds. Let (v_1, v_2) be controllers satisfying (C1)-(C3). Suppose the initial condition set Ω_0 has been selected so that for any $(\xi(0), \eta(0)) \in \Omega_0$,

$$\mathrm{e}^{\lambda_1 T^1} \|\xi(0)\| < \varepsilon_1 \quad \text{and} \quad L_\eta \varepsilon_1 < \varepsilon_2 \,.$$

Also suppose that

$$|\sqrt{2}\,\overline{\beta} + c_4 L_\alpha L_\eta | \mathrm{e}^{\lambda_1 T^\star} < 1 \tag{21}$$

where $\overline{\beta} := \max\{\beta(\eta_1), 1 \,:\, |\eta_1 - \eta_1^\star| < \varepsilon_2\}$. Then

$$\|\xi(t)\| \leq \mathrm{e}^{\lambda_1 t} \|\xi(0)\| \,, \qquad t \geq 0 \,.$$

Remark 7. The parameter ε_1 appears in (A2) while ε_2 arises in Lemma 5. To achieve $L_\eta \varepsilon_1 < \varepsilon_2$ in Lemma 6, it may be necessary to further reduce ε_1 without affecting the statement of (A2). ◁

Proof. Let $(\xi(t), \eta(t))$ be a solution of the closed-loop system (12) with $(\xi(0), \eta(0)) \in \Omega_0$ and switching times $\{t^k\}$. Notice that $|\xi_1(t^k)| = |\eta_1(t^k) + p(\eta_1(t^k))|$ since $(\xi(t^k), \eta(t^k)) \in \hat{\mathcal{S}}$. We argue by induction. For the base step: first, we have by assumption and (C3),

$$|\eta_1(t^1) + p(\eta_1(t^1))| = |\xi_1(t^1)| \leq \|\xi(t^1)\| \leq \mathrm{e}^{\lambda_1 T^1} \|\xi(0)\| < \varepsilon_1 \,.$$

Second, using the previous inequality, (A2), and by assumption,

$$|\eta_1(t^1) - \eta_1^\star| < L_\eta |\xi_1(t^1)| < L_\eta \varepsilon_1 < \varepsilon_2 \,.$$

For the induction step, suppose that

$$|\xi_1(t^k)| \leq \|\xi(t^k)\| < \varepsilon_1 \,, \quad |\eta_1(t^k) - \eta_1^\star| < \varepsilon_2 \,.$$

Now consider

$$\begin{aligned}
\|\xi(t^k)^+\| &\leq |\xi_1(t^k)^+| + |\xi_2(t^k)^+| \\
&\leq |\xi_1(t^k)| + |\beta(\eta_1(t^k))\xi_2(t^k) + \alpha(\eta_1(t^k))\eta_2(t^k)| \\
&\leq \overline{\beta}\left[|\xi_1(t^k)| + |\xi_2(t^k)|\right] + c_4 |\alpha(\eta_1(t^k))| \\
&\leq \sqrt{2}\,\overline{\beta} \|\xi(t^k)\| + c_4 L_\alpha |\eta_1(t^k) - \eta_1^\star| \\
&\leq \sqrt{2}\,\overline{\beta} \|\xi(t^k)\| + c_4 L_\alpha L_\eta |\xi_1(t^k)| \\
&\leq (\sqrt{2}\,\overline{\beta} + c_4 L_\alpha L_\eta) \|\xi(t^k)\| \\
&\leq (\sqrt{2}\,\overline{\beta} + c_4 L_\alpha L_\eta) \mathrm{e}^{\lambda_1 T^k} \|\xi(t^{k-1})^+\| \,.
\end{aligned} \tag{22}$$

The second line follows from Lemma 5 and (13b); the third line uses the definition of $\overline{\beta}$ and (C1); the fourth line uses equivalence of norms, the Lipschitz constant for $\alpha(\cdot)$, and (A4); the fifth line uses (A2); and the seventh line uses (C3). To complete the induction argument, we have

$$\begin{aligned}
|\xi_1(t^{k+1})| \leq \|\xi(t^{k+1})\| &\leq \mathrm{e}^{\lambda_1 T^{k+1}} \|\xi(t^k)^+\| \\
&\leq \mathrm{e}^{\lambda_1 T^\star} (\sqrt{2}\overline{\beta} + c_4 L_\alpha L_\eta) \|\xi(t^k)\| \\
&< \|\xi(t^k)\| < \varepsilon_1 \,.
\end{aligned}$$

The first line uses (C3); the second line uses (C1) and the sixth line of (22); the third line uses (21). Similarly,

$$\begin{aligned}
|\eta_1(t^{k+1}) - \eta_1^\star| &< L_\eta |\eta_1(t^{k+1}) + p(\eta_1(t^{k+1}))| \\
&= L_\eta |\xi_1(t^{k+1})| < L_\eta \varepsilon_1 < \varepsilon_2 \,.
\end{aligned}$$

From (22), $\|\xi(t^k)^+\| < \|\xi(t^{k-1})^+\|$. Then using (C3) and recalling the convention that $\xi(t^0)^+ = \xi(0)$, we obtain $\|\xi(t)\| \leq \mathrm{e}^{\lambda_1 t} \|\xi(0)\|$. □

At this point we have conditions ensuring that the hybrid ξ dynamics are exponentially stable. Next we examine the properties of the η dynamics to guarantee that a stable hybrid limit cycle will emerge. We begin by studying the *restricted η dynamics* given by (17) under the assumption that $\xi(t) \equiv 0$ for all $t \geq 0$. Under this assumption, the discrete reset occurs when $\eta_1 = \eta_1^\star$, and the reset map for η given in (13c)-(13d) simplifies to

$$\eta_1^+ = -\eta_1^\star \,, \qquad \eta_2^+ = \gamma^\star \eta_2 \,, \tag{23}$$

where $\gamma^\star := \gamma(\eta_1^\star)$. Let $\Omega_{0,\eta} \subset \mathcal{P}$ be the maximal set of initial conditions in $\mathcal{P}$ such that solutions of the restricted system remain in $\mathcal{P}$ (this set can be computed analytically based on the simplicity of the dynamics). We begin by establishing the existence of a hybrid limit cycle for the restricted η dynamics.

Lemma 8. Consider the restricted hybrid system (17) and (23). Suppose $\gamma^\star > 0$. For every initial condition $\eta_0 \in \Omega_{0,\eta}$, the positive limit set is a hybrid limit cycle.

Proof. The proof mimics that of the standard Poincaré-Bendixson theorem; we focus on the differences to address the reset map. Consider any $\eta_0 \in \Omega_{0,\eta}$. Since $\mathcal{P}$ is compact, by a minor variation of Birkhoff's theorem the positive limit set $L^+(\eta_0)$ is non-empty, compact, and invariant. Additionally, $\lim_{t\to 0} d_{L^+(\eta_0)}(\eta(t)) = 0$. Consider the cross-section $\mathcal{V}^+$ in (20) and the sequence of points $\{p^k\}$, where $p^0 := \eta_0$, $p^k = (p_1^k, p_2^k) := \eta(t^k)^+ \in \mathcal{V}^+$, and $\{t^k\}$ is the sequence of switching times for $k \geq 1$. We claim $\{p^k\}$ is monotone along $\mathcal{V}^+$ for $k \geq 1$. Let $p^1 \in \mathcal{V}^+$, and consider the solution $\eta(t)$ over the time interval $[t^1, t^2]$, forming a continuous curve $\mathcal{C}_{12}$. The solution reaches a point $\eta(t^2) = (\eta_1^\star, \eta_2(t^2))$ when it is reset to $p^2 = (-\eta_1^\star, \gamma^\star \eta_2(t^2))$. First suppose $p_2^2 > p_2^1$. Then the next solution curve $\mathcal{C}_{23}$ lies entirely above the curve $\mathcal{C}_{12}$, since the latter cannot be crossed (by uniqueness of solutions). This means that at t^3, the time of the next discrete step, we have $\eta_2(t^3) > \eta_2(t^2)$ so that $p_2^3 = \gamma^\star \eta_2(t^3) > \gamma^\star \eta_2(t^2) = p_2^2$. This argument can be repeated to obtain a monotone sequence on $\mathcal{V}^+$. Instead, suppose $p_2^2 \leq p_2^1$. Then the next solution curve $\mathcal{C}_{23}$ lies entirely on or below the curve $\mathcal{C}_{12}$. At the next discrete step, $\eta_2(t^3) \leq \eta_2(t^2)$, so $p_2^3 = \gamma^\star \eta_2(t^3) \leq \gamma^\star \eta_2(t^2) = p_2^2$. Again, we obtain a monotone sequence on $\mathcal{V}^+$. The remainder of the proof follows the steps of the Poincaré-Bendixson theorem: $L^+(\eta_0) \cap \mathcal{V}^+$ is a single point; for every $p \in L^+(\eta_0)$, the positive orbit $O^+(p)$ is a hybrid limit cycle $\mathcal{O}$; finally, $L^+(\eta_0) = \mathcal{O}$. We omit these steps which closely mimic the standard proof. □

Lemma 9. Consider the restricted hybrid system (17) and (23). Define $\mathcal{P}^+ = \{\eta \in \mathcal{P} \mid \eta_2 \geq -g/K_2\}$. If $0 < \gamma^\star < 1$, then all solutions of the restricted system starting in $\mathcal{P}$ eventually reach $\mathcal{P}^+$.

Proof. If $\eta(0) \in \mathcal{P}^+$, we are done. Suppose instead $\eta_2(0) < -g/K_2$. Since $d_{\mathcal{W}}(\eta(t)) = \mathrm{e}^{K_2 t} d_{\mathcal{W}}(\eta(t^k)^+)$ over each continuous interval $t \in [t^{k+1}, t^k]$, and since $0 <$

$\gamma^\star < 1$, there exists k sufficiently large such that $\eta_2(t^k) < -g/K_2$ and $\gamma^\star \eta_2(t^k) > -g/K_2$. □

Consider the cross section $\mathcal{V}^+$ given in (20) and define the Poincaré map $f : \mathcal{V}^+ \to \mathcal{V}^+$ by

$$f(\eta_0) := \eta(\tau(\eta_0))^+ = (-\eta_1^\star, \gamma^\star \eta_2(\tau(\eta_0))) \,, \tag{24}$$

where $\eta(t)$ is a solution of the restricted system, $\eta(0) = \eta_0 \in \mathcal{V}^+$, and $\tau(\eta_0)$ is the first time the solution reaches $\mathcal{V}^-$. Lemma 8 tells us that each bounded solution of (17) tends to a hybrid limit cycle. Each such hybrid limit cycle corresponds to a fixed point of the Poincaré map. Next we prove that the Poincaré map has only one stable fixed point. Therefore the system (17) admits a unique stable hybrid limit cycle.

Theorem 10. Suppose $0 < \gamma^\star < 1$. Then the restricted hybrid system (17) and (23) has a unique stable hybrid limit cycle.

Proof. Consider the Poincaré section $\mathcal{V}^+$ in $\mathcal{P}$ and the Poincaré map $f : \mathcal{V}^+ \to \mathcal{V}^+$ in (24). Consider any two solutions $\eta(t)$ and $\eta'(t)$ of the restricted system with $\eta(0), \eta'(0) \in \Omega_{0,\eta}$. In light of Lemma 9, we assume w.l.o.g. that $\eta(t^k)^+, \eta'(\tau^k)^+ \in \mathcal{P}^+$ where $\{t^k\}$ and $\{\tau^k\}$ are the discrete switching times of each solution. Also, w.l.o.g. assume $\eta_2(t^k)^+ > \eta_2'(\tau^k)^+$. Then

$$\|\eta(t^k)^+ - \eta'(\tau^k)^+\| = d_{\mathcal{W}}(\eta(t^k)^+) - d_{\mathcal{W}}(\eta'(\tau^k)^+) \,.$$

By (18), we have

$$\left\|\eta(t^{k+1}) - \eta'(\tau^{k+1})\right\| = \mathrm{e}^{K_2 T} d_{\mathcal{W}}(\eta(t^k)^+) - \mathrm{e}^{K_2 T'} d_{\mathcal{W}}(\eta'(\tau^k)^+)$$

where $T = t^{k+1} - t^k$ and $T' = \tau^{k+1} - \tau^k$. By (19) we know that $T \geq T'$. Thus,

$$\begin{aligned}\left\|\eta(t^{k+1}) - \eta'(\tau^{k+1})\right\| &\leq \mathrm{e}^{K_2 T'} \left\|\eta(t^k)^+ - \eta'(\tau^k)^+\right\| \\ &\leq \mathrm{e}^{K_2 T^\star} \left\|\eta(t^k)^+ - \eta'(\tau^k)^+\right\| \,.\end{aligned}$$

When the reset map is applied, we have

$$\begin{aligned}\|\eta(t^{k+1})^+ - \eta'(\tau^{k+1})^+\| &= \gamma^\star \|\eta(t^{k+1}) - \eta'(\tau^{k+1})\| \\ &\leq \gamma^\star \mathrm{e}^{K_2 T^\star} \|\eta(t^k)^+ - \eta'(\tau^k)^+\| \,.\end{aligned} \tag{25}$$

Since by assumption $0 < \gamma^\star < 1$, we have $0 < \gamma^\star \mathrm{e}^{K_2 T^\star} < 1$, so (25) defines a contraction mapping on $\mathcal{V}^+$. This implies that the Poincaré map has a unique fixed point, by the Banach fixed point theorem. Further, this fixed point is asymptotically stable. Finally, we invoke Proposition 2, p. 283 of (Hirsch and Smale, 1974) to conclude that the hybrid limit cycle associated with the stable fixed point is itself asymptotically stable. □

Remark 11. The condition $\gamma^\star < 1$ is not necessary, and one can prove existence of a stable hybrid limit cycle using the more relaxed condition $0 < \gamma^\star \mathrm{e}^{K_2 T^\star} < 1$. On the other hand, the stricter condition simplifies our proof so we have given precedence to brevity over generality here. ◁

Finally, we return to the full hybrid system.

Theorem 12. Consider the hybrid system (12), and suppose that Assumption 1 holds. Let (v_1, v_2) be controllers satisfying (C1)-(C3). Let $\Omega_0 \subset \mathcal{P}$ satisfy the conditions of Lemma 6 and suppose (21) holds. If $0 < \gamma^\star < 1$, then the closed-loop system exhibits a unique stable hybrid limit cycle.

Proof. The VHC is controlled invariant by Assumptions (A3) and (A4). This implies the stable hybrid limit cycle of the restricted dynamics (17)-(23) is also a hybrid limit cycle of the full hybrid system (12). Then the fixed point argument of Theorem 10 can then be extended to the full system. See the proof of Theorem 4.6 in (Westervelt et al., 2007) for the details. □

7. DESIGN PROCEDURE AND SIMULATIONS

Our theoretical results suggest the following procedure.

(D1) Choose the VHC to satisfy Assumption 1.
(D2) Compute $\gamma^\star$ and $T^\star$ and verify that $0 < \gamma^\star < 1$.
(D3) Design $v_2(\eta)$ based on a reach control approach such that (C2) holds. A sample controller is (16).
(D4) Design $v_1(\xi)$ using pole placement such that (C1) and (21) hold. In practice, (21) is met by choosing $\lambda_1 < 0$ sufficiently negative.
(D5) Obtain an estimate of Ω_0 by (analytically) computing $\Omega_{0,\eta}$ for the restricted hybrid system (17) and (23). Fine tune the estimate for Ω_0 using a simulation of the full system.
(D6) Iterate on (D3) to adjust up or down the gait speed by moving the location of the affine invariant space $\mathcal{W}$ induced by $v_2(\eta)$.

We simulated the robot in Figure 1 with parameters $m_1 = m_2 = 5$Kg and $m_H = 10$Kg. The length of each leg is 1m with the center of mass at the middle of each leg. We chose $\eta_2 \in [-0.25, -1]$ m/s for the safety and liveness constraints on η_2, based on similar constraints for the Cassie robot (Gong et al., 2019). For the safety constraint on the size of a step of the stance leg, we chose $|\eta_1| \leq 0.8$ rad, corresponding to slightly more than 45 deg. The shape of the gait is chosen as in Figure 2, where $p(q_1) = 6.8q_1^3 - 0.476q_1^2 - 1.83q_1 + 0.0584$. For this choice of p we obtain $\eta_1^\star = -0.35$. Next, we select the PD controller $v_1 = -200\xi_1 - 31\xi_2$ to stabilize the ξ dynamics. Finally, we use the reach controller $v_2 = -2.4\eta_2 - 1.4$ to achieve the desired behavior on $\mathcal{P}$, as depicted in Figure 3. With these choices of controllers, we compute $\lambda_1 = -9.0845$, $K_2 = -2.4$, and $T^\star = 1.3389$s. Finally, we verify that $\gamma^\star = 0.6618 < 1$ for the selected VHC, thus satisfying the requirement of Theorem 12.

Figure 3 shows the phase portrait for the η-dynamics. The blue curve corresponds to the hybrid limit cycle. The green region corresponds to the set of initial conditions for which solutions converge to the hybrid limit cycle, assuming that $\xi(0) = (1, 10)$. Note, that this choice of initial condition for $\xi(0)$ is taken to be particularly large (the legs are nearly 60 degrees out of phase with the VHC) to show that convergence to the desired steady-state behavior occurs for a large set of initial conditions in $\mathcal{P}$.

8. CONCLUSION

Inspired by reach control theory, we have demonstrated a simple controller for guaranteed regulation of the gait speed of a walking robot. Our method can be effective for safely transitioning between gaits. This is because the positively invariant set $\Omega_{0,\eta} \subset \mathcal{P}$ can be computed analytically, and it provides a good approximation for the η part of initial condition set Ω_0 for the full hybrid dynamics. This means one may verify that at the end of one or two steps, the state of the robot lies inside the

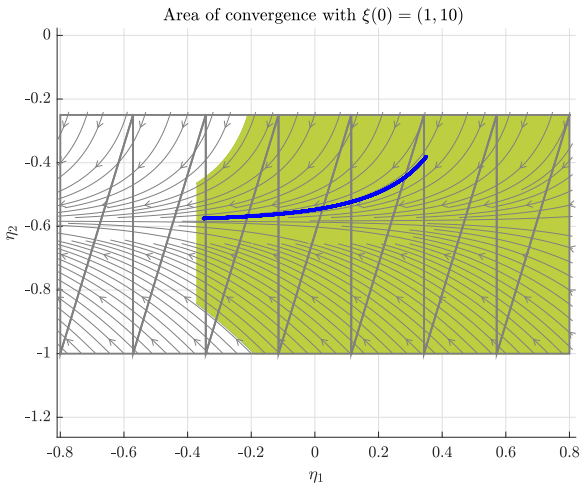

Fig. 3. Phase portrait of the closed-loop η dynamics. The closed-loop poles of the ξ dynamics are $\{-22, -9\}$ and the initial condition is $\xi(0) = (1, 10)$. The blue curve is the hybrid limit cycle and the green region shows its domain of attraction projected to $\mathcal{P}$.

initial condition set Ω_0' for the next gait. A potentially useful extension is to use piecewise affine controllers for v_2 to shape the profile of the gait speed over a single gait cycle.

REFERENCES

Agrawal, A. and Sreenath, K. (2019). Bipedal robotic running on stochastic discrete terrain. In *European Control Conference*.

Al Lawati, M. and Yousef, H. (2016). Stability analysis and trajectory design of a 2-dof bipedal walker. In *IEEE Canadian Conf. Elec. Comp. Engin.*, 1–5.

Broucke, M.E. (2010). Reach control on simplices by continuous state feedback. *SIAM J. Control and Optimization*, 48(5), 3482–3500.

Clark, W. and Bloch, A. (2018). Stable orbits for a simple passive walker experiencing foot slip. In *IEEE Conf. Decision and Control*, 2366–2371.

Da, X., Harib, O., Hartley, R., Griffin, B., and Grizzle, J. (2016). From 2d design of underactuated bipedal gaits to 3d implementation: Walking with speed tracking. *IEEE Access*, 4, 3469–3478.

Freidovich, L.B., Mettin, U., Shiriaev, A.S., and Spong, M.W. (2008). A passive 2DOF walker: Finding gait cycles using virtual holonomic constraints. In *IEEE Conf. Decision and Control*, 5214–5219.

Gong, Y., Hartley, R., Da, X., Hereid, A., Harib, O., Huang, J., and Grizzle, J.W. (2019). Feedback control of a cassie bipedal robot: Walking, standing, and riding a segway. In *American Control Conference*.

Grizzle, J., Abba, G., and Plestan, F. (2001). Asymptotically stable walking for biped robots: Analysis via systems with impulse effects. *IEEE Trans. Automatic Control*, 46(1), 51–64.

Habets, L.C.G.J.M., Collins, P.J., and van Schuppen, J.H. (2006). Reachability and control synthesis for piecewise-affine hybrid systems on simplices. *IEEE Trans. Automatic Control*, 51(6), 938–948.

Helwa, M.. and Broucke, M.E. (2013). Monotonic reach control on polytopes. *IEEE Trans. Automatic Control*, 58, 2704–2709.

Hirsch, M. and Smale, S. (1974). *Differential Equations, Dynamical Systems, and Linear Algebra*. Academic Press.

Kloetzer, M. and Belta, C. (2008). A fully automated framework for control of linear systems from temporal logic specifications. *IEEE Trans. Automatic Control*, 53, 287–297.

Manchester, I., Tobenkin, M., Levashov, M., and Tedrake, R. (2010). Regions of attraction for hybrid limit cycles of walking robots. *IFAC Proceedings*, 44, 5801–5806.

Otsason, R. and Maggiore, M. (2019). On the generation of virtual holonomic constraints for mechanical systems with underactuation degree one. In *IEEE Conf. Decision and Control*.

Roszak, B. and Broucke, M.E. (2006). Necessary and sufficient conditions for reachability on a simplex. *Automatica*, 42(11), 1913–1918.

Westervelt, E., Grizzle, J., and Koditschek, D. (2002). Zero dynamics of underactuated planar biped walkers. In *IFAC World Congress*.

Westervelt, E., Grizzle, J., Chevallereau, C., Choi, J.H., and Morris, B. (2007). *Feedback control of dynamic bipedal robot locomotion*. CRC Press.

Westervelt, E.R., Grizzle, J.W., and Koditschek, D.E. (2003). Hybrid zero dynamics of planar biped walkers. *IEEE Trans. Automatic Control*, 48(1), 42–56.

Appendix A.

Proof. From (A2), (A3), (13a), and (13c), there exists $(\xi^\star, \eta^\star) \in \hat{\mathcal{S}} \cap \hat{\Gamma}$ such that $(\xi_1^\star)^+ = 0$ and $(\eta_1^\star)^+ = -\eta_1^\star = p(\eta_1^\star)$. Now consider any $(\xi, \eta) \in \hat{\mathcal{S}}$. Applying Taylor's theorem, we have

$$\begin{aligned}\xi_1 &= -\eta_1 - p(\eta_1)\\ &= -\eta_1 - p(\eta_1^\star) - \frac{\partial p}{\partial \eta_1}\Big|_{\eta_1^\star}(\eta_1 - \eta_1^\star) + o(\eta_1 - \eta_1^\star)\\ &= -\left(1 + \frac{\partial p}{\partial \eta_1}\Big|_{\eta_1^\star}\right)(\eta_1 - \eta_1^\star) + o(\eta_1 - \eta_1^\star),\end{aligned} \tag{A.1}$$

where $\lim_{z\to 0} \frac{o(z)}{z} = 0$. Similarly, starting from (13a), we compute

$$\begin{aligned}\xi_1^+ &= \eta_1 - p(-\eta_1) = \eta_1 - p(\eta_1^+)\\ &= \eta_1 - p((\eta_1^\star)^+) - \frac{\partial p}{\partial \eta_1}\Big|_{(\eta_1^\star)^+}\left(\eta_1^+ - (\eta_1^\star)^+\right) + o(\eta_1^+ - (\eta_1^\star)^+)\\ &= \eta_1 + p(\eta_1^\star) + \frac{\partial p}{\partial \eta_1}\Big|_{(\eta_1^\star)^+}(\eta_1 - \eta_1^\star) + o(\eta_1 - \eta_1^\star)\\ &= \eta_1 - \eta_1^\star + \frac{\partial p}{\partial \eta_1}\Big|_{(\eta_1^\star)^+}(\eta_1 - \eta_1^\star) + o(\eta_1 - \eta_1^\star)\\ &= \left(1 + \frac{\partial p}{\partial \eta_1}\Big|_{-\eta_1^\star}\right)(\eta_1 - \eta_1^\star) + o(\eta_1 - \eta_1^\star).\end{aligned} \tag{A.2}$$

Comparing (A.1) and (A.2), we see that there exists $\epsilon_2 > 0$ such that with $|\eta_1 - \eta_1^\star| < \epsilon_2$ and by (A5), we obtain $|\xi_1^+| < |\xi_1|$, as desired. □